amount of ERα46 transcripts was too little to evaluate the correlation with the clinicopathological factors of ERα+ breast cancer.

In this study, we found out that *ERα* transcription used the same promoter choice as promoter A, which was significantly ($P < .05$) associated with mRNA expression of the *ERα* gene in individual breast cancer.

Conclusion

We have investigated the transcriptional regulation of *ERα*, but the mechanism of the regulation remains to be discovered. In this article, we reinvestigated variations in the use of > 3 *ERα* promoters in breast cancer tissues and breast cancer cell lines with an eye toward using *ERα* promoter usage as a new biomarker, and found that the *ERα* promoter usage of ERα$^+$ breast cancer tissues and cell lines were similar, and the similarity was validated by examinations using correlation among transcripts from each promoter and that of total *ERα* and relation to clinicopathological factors. Although the likelihood of using *ERα* promoter usage in breast cancer tissues as a clinical biomarker was small, this article is meaningful in presenting the possibility that *ERα* promoter usage might be important for individual development, differentiation, or carcinogenesis, and that the biological meaning of *ERα* promoter usage could be discovered by comparison of the promoter usage in breast cancer cell lines with the promoter usage of other cancer tissues with ERα positivity.

Clinical Practice Points

- The *ERα* gene has at least 6 transcription start sites and 6 distinct first exons. It also probably has 6 promoters, which is unusual for functionally discovered nuclear receptors.
- Typical tissue promoter usages in cancer cell lines and normal tissues were found, using an ERE luciferase assay and quantification of promoter-specific mRNA of *ERα*.
- In this article, we investigated *ERα* promoter usage in individual breast cancer with an eye toward using *ERα* promoter usage as a new biomarker, using a real-time PCR method with primers and probes designed especially for this assay. We found that the *ERα* promoter usages of ERα$^+$ breast cancer tissues and cell lines were similar, and the similarity was validated by examinations using correlation among transcripts from each promoter and that of total *ERα* and relation to clinicopathological factors.
- Although the likelihood of using *ERα* promoter usage in breast cancer tissues as a clinical biomarker was small, this article is meaningful in presenting the possibility that *ERα* promoter usage might be important for individual development, differentiation, or carcinogenesis.

Disclosure

The authors have stated that they have no conflicts of interest.

References

1. Early Breast Cancer Trialists' Collaborative Group (EBCTCG). Effects of chemotherapy and hormonal therapy for early breast cancer on recurrence and 15-year survival: an overview of the randomised trials. *Lancet* 2005; 365:1687-717.
2. Forbes JF, Cuzick J, Baum M, et al. Effect of anastrozole and tamoxifen as adjuvant treatment for early-stage breast cancer: 100-month analysis of the ATAC trial. *Lancet Oncol* 2008; 9:45-53.
3. Thürlimann B, Keshaviah A, Goldhirsch A, et al. A comparison of letrozole and tamoxifen in postmenopausal women with early breast cancer. *N Engl J Med* 2005; 353:2747-57.
4. van de Velde CJ, Rea D, Jones SE, et al. Adjuvant tamoxifen and exemestane in early breast cancer (TEAM): a randomised phase 3 trial. *Lancet* 2011; 377:321-31.
5. Gohno T, Seino Y, Hayashi S, et al. Individual transcriptional activity of estrogen receptors in primary breast cancer and its clinical significance. *Cancer Med* 2012; 1:328-37.
6. Tanimoto K, Eguchi H, Hayashi S, et al. Regulation of estrogen receptor alpha gene mediated by promoter B responsible for its enhanced expression in human breast cancer. *Nucleic Acids Res* 1999; 27:903-9.
7. Yoshida T, Eguchi H, Hayashi S, et al. Distinct mechanisms of loss of estrogen receptor alpha gene expression in human breast cancer: methylation of the gene and alteration of trans-acting factors. *Carcinogenesis* 2000; 21:2193-201.
8. Hayashi S, Imai K, Nakachi K, et al. Two promoters in expression of estrogen receptor messenger RNA in human breast cancer. *Carcinogenesis* 1997; 18:459-64.
9. Inoue A, Hayashi S, Kiyama R, et al. A reporter gene assay for evaluation of tissue-specific responses to estrogens based on the differential use of promoters A to F of the human estrogen receptor alpha gene. *J Pharmacol Toxicol Methods* 2002; 47: 129-35.
10. Tang Z, Treilleux I, Brown M, et al. A transcriptional enhancer required for the differential expression of the human estrogen receptor in breast cancers. *Mol Cell Biol* 1997; 17:1274-80.
11. McPherson LA, Baichwal VR, Weigel RJ, et al. Identification of ERF-1 as a member of the AP2 transcription factor family. *Proc Natl Acad Sci USA* 1997; 94: 4342-7.
12. Treilleux I, Peloux N, Sergeant A, et al. Human estrogen receptor (ER) gene promoter-P1: estradiol-independent activity and estradiol inducibility in ER$^+$ and ER$^-$ cells. *Mol Endocrinol* 1997; 11:1319-31.
13. Schuur ER, McPherson LA, Weigel RJ, et al. Genomic structure of the promoters of the human estrogen receptor-alpha gene demonstrate changes in chromatin structure induced by AP2gamma. *J Biol Chem* 2001; 276:15519-26.
14. Walter P, Green S, Waterfield M, et al. Cloning of the human estrogen receptor cDNA. *Proc Natl Acad Sci USA* 1985; 82:7889-93.
15. Grandien K. Determination of transcription start sites in the human estrogen receptor gene and identification of a novel, tissue-specific, estrogen receptor-mRNA isoform. *Mol Cell Endocrinol* 1996; 116:207-12.
16. Thompson DA, McPherson LA, Weigel RJ, et al. Identification of two estrogen receptor transcripts with novel 5' exons isolated from a MCF7 cDNA library. *J Steroid Biochem Mol Biol* 1997; 62:143-53.
17. Flouriot G, Griffin C, Gannon F, et al. Differentially expressed messenger RNA isoforms of the human estrogen receptor-alpha gene are generated by alternative splicing and promoter usage. *Mol Endocrinol* 1998; 12:1939-54.
18. Kos M, Reid G, Gannon F, et al. Minireview: genomic organization of the human ERalpha gene promoter region. *Mol Endocrinol* 2001; 15:2057-63.
19. Kastner P, Krust A, Chambon P, et al. Two distinct estrogen-regulated promoters generate transcripts encoding the two functionally different human progesterone receptor forms A and B. *EMBO J* 1990; 9:1603-14.
20. Dehm SM, Tindall DJ. Alternatively spliced androgen receptor variants. *Endocr Relat Cancer* 2011; 18:R183-96.
21. Grandien K, Bäckdahl M, Berkenstam A, et al. Estrogen target tissue determines alternative promoter utilization of the human estrogen receptor gene in osteoblasts and tumor cell lines. *Endocrinology* 1995; 136:2223-9.
22. Amaral S, Schroth W, Brauch H, et al. The promoter C specific ERalpha isoform is associated with tamoxifen outcome in breast cancer. *Breast Cancer Res Treat* 2009; 118:323-31.
23. Harvey JM, Clark GM, Allred DC, et al. Estrogen receptor status by immunohistochemistry is superior to the ligand-binding assay for predicting response to adjuvant endocrine therapy in breast cancer. *J Clin Oncol* 1999; 17:1474-81.
24. Osterlund MK, Grandien K, Hurd YL, et al. The human brain has distinct regional expression patterns of estrogen receptor alpha mRNA isoforms derived from alternative promoters. *J Neurochem* 2000; 75:1390-7.
25. Ishii H, Kobayashi M, Sakuma Y, et al. Alternative promoter usage and alternative splicing of the rat estrogen receptor alpha gene generate numerous mRNA variants with distinct 5'-ends. *J Steroid Biochem Mol Biol* 2010; 118:59-69.
26. Hamada T, Wada-Kiyama Y, Sakuma Y. Visualizing forebrain-specific usage of an estrogen receptor alpha promoter for receptor downregulation in the rat. *Brain Res Mol Brain Res* 2005; 139:42-51.
27. Flouriot G, Brand H, Gannon F, et al. Identification of a new isoform of the human estrogen receptor-alpha (HER-alpha) that is encoded by distinct transcripts and that is able to repress HER-alpha activation function 1. *EMBO J* 2000; 19: 4688-700.
28. Wang Z, Zhang X, Deuel T, et al. Identification, cloning, and expression of human estrogen receptor-alpha36, a novel variant of human estrogen receptor-alpha66. *Biochem Biophys Res Commun* 2005; 336:1023-7.
29. Klinge CM, Riggs KA, Magnusen JE, et al. Estrogen receptor alpha 46 is reduced in tamoxifen resistant breast cancer cells and re-expression inhibits cell proliferation and estrogen receptor alpha 66-regulated target gene transcription. *Mol Cell Endocrinol* 2010; 323:268-76.
30. Shi L, Dong B, Li Z, et al. Expression of ER-{alpha}36, a novel variant of estrogen receptor {alpha}, and resistance to tamoxifen treatment in breast cancer. *J Clin Oncol* 2009; 27:3423-9.

Supplemental Table 1 The Sequence of Primers and Probes Used in This Study

Primer List	Sequence (5'→3')
ERα Promoter A Forward Primer (F1)	CTGTGCTCTTTTTCCAGGTG
ERα Promoter B Forward Primer (F2)	CAGCGACGACAAGTAAAGTG
ERα Promoter C Forward Primer (F3)	GTTCTTGATCCAGCAGGGTG
ERα Promoter D Forward Primer (F4)	CACCTGAGAGAGCCAGTG
ERα Promoter Common Reverse Primer (R1)	AGGGTCATGGTCATGGTC
ERα Promoter E Forward Primer (F5)	ACCAATCCTTTTGATTGTGAA
ERα Promoter F Forward Primer (F6)	GCATAAGAAGACAGTCTCTGAGTGA
ERα Promoter Common Reverse Primer (R2)	GGCAGAAGGCTCAGAAACC
ERα Promoter Common Probe (P1)	CCGGTTTCTGAGCCTTCTGCCC
ERα Promoter Common Probe (P2)	ACATTCTCCGGGACTGCGGTACCA
Total ERα Exon7 Forward Primer (F7)	CTCCCACATCAGGCACAT
Total ERα Exon8 Reverse Primer (R3)	CTCCAGCAGCAGGTCATA

Supplemental Figure 1 **Analyses of ER Alpha Variants With This Promoter-Specific Method. (A) Exon Structure of the ERα Variant ERα46. This Messenger RNA (mRNA) Originates From the Same Promoters, E and F, as Those of Normal *ERα* Gene. Two 5′-UTR Exons of This mRNA Were Directly Spliced to Exon 2, but not to Exon 1. (B) The Real-Time Polymerase Chain Reaction Analysis of *ERα46* Transcripts. The Amount of *ERα46* Transcripts Originating From Both Promoter E and F was Normalized to That of the Transcripts From Promoter A. The Horizontal Axis Indicates the Identification Number of Breast Cancer Samples and Vertical Axis Indicates the Levels of Transcripts Originating From Both Promoter E and F, Relative to Those Originating From Promoter A. (C) The Sequence of the Reverse Primer Designed for the Analysis of *ERα46***

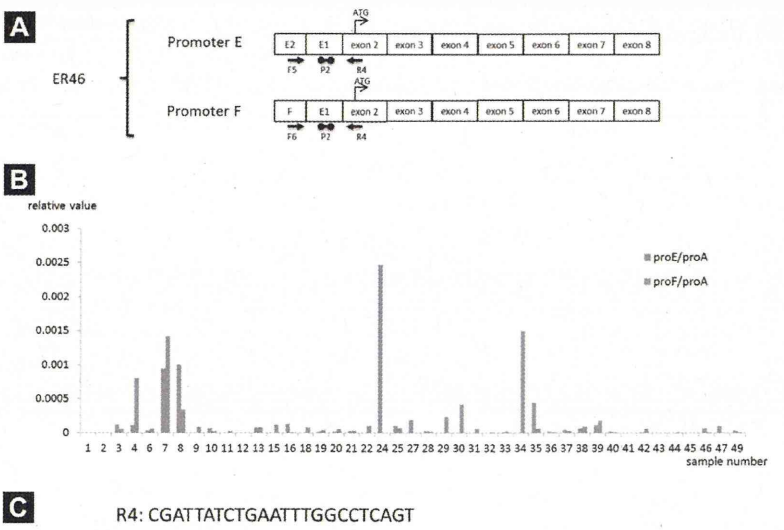

Abbreviations: proA = promoter A; proE = promoter E; proF promoter F.

Biochemical and Biophysical Research Communications 443 (2014) 1148–1154

Contents lists available at ScienceDirect

Biochemical and Biophysical Research Communications

journal homepage: www.elsevier.com/locate/ybbrc

Centrosomal BRCA2 is a target protein of membrane type-1 matrix metalloproteinase (MT1-MMP)

Nadila Wali [a,d], Kana Hosokawa [a], Sadiya Malik [a], Hiroko Saito [b], Ken Miyaguchi [a], Shinobu Imajoh-Ohmi [c], Yoshio Miki [a,b,*], Akira Nakanishi [a]

[a] Department of Molecular Genetics, Medical Research Institute, Tokyo Medical and Dental University (TMDU), Japan
[b] Department of Molecular Diagnosis, Cancer Institute, The Japanese Foundation of Cancer Research (JFCR), Japan
[c] Medical Proteomics Laboratory, The Institute of Medical Science, The University of Tokyo, Japan
[d] Department of Obstetrics and Gynecology, Urumqi Friendship Hospital, Xinjiang, PR China

ARTICLE INFO

Article history:
Received 6 December 2013
Available online 30 December 2013

Keywords:
BRCA2
MT1-MMP
Centrosome

ABSTRACT

BRCA2 localizes to centrosomes between G1 and prophase and is removed from the centrosomes during mitosis, but the underlying mechanism is not clear. Here we show that BRCA2 is cleaved into two fragments by membrane type-1 matrix metalloproteinase (MT1-MMP), and that knockdown of MT1-MMP prevents the removal of BRCA2 from centrosomes during metaphase. Mass spectrometry mapping revealed that the MT1-MMP cleavage site of human BRCA2 is between Asn-2135 and Leu-2136 (^{2132}LSNN/LNVEGG^{2141}), and the point mutation L2136D abrogated MT1-MMP cleavage. Our data demonstrate that MT1-MMP proteolysis of BRCA2 regulates the abundance of BRCA2 on centrosomes.

1. Introduction

Germline mutations of BRCA2 (breast cancer type 2 susceptibility gene) that truncate the encoded protein result in increased predisposition to cancers of the breast, ovaries [1], and pancreas [2]. Although the role of BRCA2 inactivation in sporadic carcinogenesis remains unclear, several studies have provided evidence that loss of BRCA2 facilitates cancer cell proliferation [3]. BRCA2 is a large protein consisting of 3418 amino acids, including a nuclear localization signal (NLS), centrosomal localization signal (CLS), and nuclear export sequence (NES), and plays multiple roles in repair of DNA double-stand breaks (DSBs), centrosome replication [4], and cytokinesis [5]. In human cell lines, the level of BRCA2 is regulated throughout the cell cycle: expression is low in G0 and G1 phase, but increases as the cell enters S phase [6].

Tight control of cell-cycle progression is ensured by multiple mechanisms, including ubiquitination of G1 cyclin and CDK inhibitors. For example, Skp2 targets numerous substrates such as p27 [7] and BRCA2 for degradation [8]. Previous studies have shown that BRCA2 is localized to the centrosomes during interphase and prophase, but not after prophase [4]. The mechanism by which BRCA2 is removed from the centrosomes during mitosis is not yet clear; to date, ubiquitinated BRCA2 has not been detected at centrosomes. Changes in protein levels over the course of the cell cycle are regulated by ubiquitin-independent proteolysis as well as by the ubiquitin–proteasome system. Several proteolytic activities have been localized to centrosomes, including MT1-MMP, initially described for its role in proteolytic cleavage of the membrane-tethered MMP subfamily [9]. Although best known for its pericellular activities, endocytosed MT1-MMP has also been shown to traffic to the centrosome [10], where it cleaves centrosomal pericentrin. Furthermore, MT1-MMP has been reported to exhibit the preference of cleavage sites [11]. The *MEROPS* database (http://merops.sanger.ac.uk/) includes a collection of known cleavage sites in protease substrates [12,13].

Here, we provide compelling evidence that BRCA2 is cleaved by MT1-MMP. MT1-MMP-depleted cells exhibited elevated levels of wild-type BRCA2 and reduced levels of BRCA2 cleavage. Furthermore, BRCA2 exhibited centrosomal localization during metaphase in MT1-MMP-depleted cells. Finally, expression of wild-type BRCA2 was inversely correlated with the level of BRCA2 cleavage over the course of the cell cycle. Taken together, these results demonstrate that the abundance of BRCA2 protein on centrosomes is controlled by MT1-MMP.

2. Materials and methods

2.1. Plasmid and antibodies

FLAG-tagged BRCA2 protein was generated by fusing sequence encoding the FLAG epitope to the 3′ end of the BRCA2 gene, thereby

* Corresponding author at: Department of Molecular Genetics, Medical Research Institute, Tokyo Medical and Dental University, 1-5-45, Yushima, Bunkyo-ku, Tokyo 113-8510, Japan. Fax: +81 3 5803 5828.
E-mail address: miki.mgen@mri.tmd.ac.jp (Y. Miki).

0006-291X/$ - see front matter © 2013 Elsevier Inc. All rights reserved.
http://dx.doi.org/10.1016/j.bbrc.2013.12.103

creating gene encoding the BRCA2 protein with a carboxy-terminal FLAG tag. GST-tagged BRCA2 (amino acids [a.a.] 1968–2135) protein was generated by fusing sequence encoding GST to the 5′ end of the BRCA2 gene, thereby creating a gene encoding the BRCA2 protein with an N-terminal GST tag. HA-tagged BRCA2 (a.a. 1596–2280) protein was generated by fusing sequence encoding the HA epitope 5′ to BRCA2 gene, thereby creating gene encoding the BRCA2 protein with an N-terminal HA tag. The following commercially available antibodies were used in this study: anti-BRCA2 rabbit polyclonal antibody (pAb) (Ab123491, Abcam, Cambridge, UK); anti-BRCA2 mouse monoclonal antibody (mAb) (Ab-1, Calbiochem); anti-BRCA2 rabbit pAb (H-300 and H-299, Santa Cruz Biotechnology, Dallas, TX, USA); anti-HA rat mAb (3F10, Cell Signaling Technology, Danvers, MA, USA); anti-FLAG mAb (F3165, Sigma–Aldrich, St. Louis, MO, USA); anti-BRCA2 rabbit pAb (5.23, Merck Millipore, Billerica, MA, USA); anti-MT1-MMP [LEM-2/63.1] catalytic domain mouse mAb (ab78738, Abcam); anti-β-actin mAb (AC-74, Sigma–Aldrich); anti-PCNA mAb (5A10, MBL, Nagoya, Japan).

2.2. Peptide synthesis and antibody preparation

Peptides were synthesized by the solid-phase method on an Applied Biosystems Model 430A peptide synthesizer, and purified by reverse-phase high performance liquid chromatography on a C18 column. The following antibodies were generated in rabbits, using synthetic peptides as haptens conjugated to keyhole limpet hemocyanin (KLH), and purified from antisera by affinity chromatography using immobilized antigen peptides: brca2n, which recognizes the N-terminal cleavage fragment of BRCA2, raised against residues 2126–2135 (CSKEFKLSNN); and brca2c, which recognizes the C-terminal cleavage fragment of BRCA2, raised against residues 2136–2149 (LNVEGGSSENNHSI). Antibody titer in antiserum was monitored by dot-blot assay. When the antibody titer increased sufficiently, rabbits were bled from the ear artery (30–50 ml).

2.3. Cell culture and transfection

HeLa S3 cells were purchased from the RIKEN GenBank (Ibaraki, Japan) and cultured in Dulbecco's Modified Eagle Medium (DMEM; Nissui Pharmaceutical, Tokyo, Japan) supplemented with 10% fetal bovine serum (FBS). Other cell lines, U2OS cells, and MCF7 cells were obtained from ATCC (Manassas, VA, USA). HA-BRCA2 and BRCA2-FLAG were expressed into HeLa S3 cells. HeLa S3 cells were synchronized in S phase by a double-thymidine block (DTB): cells were incubated in 2.5 mM thymidine for 18 h, washed with PBS, released for 9 h, and then blocked for another 15 h in 2.5 mM thymidine.

2.4. Immunoblotting and immunoprecipitation (IP) analysis

Anti-normal rabbit IgG or anti-BRCA2 antibody was added to the HeLa S3 cells extract and incubated for 30 min at 4 °C with shaking. Protein G-Sepharose (20 μl of 50% suspension) was added, and the mixture was further incubated for 1 h at 4 °C with shaking. Immunoprecipitates were washed five times with cell lysis buffer containing protease inhibitors. After washing, samples were subjected to SDS–PAGE and transferred electrophoretically onto 0.45-μm PVDF membranes (Merck Millipore). The membranes were stained with primary antibodies for 2 h at RT, followed by incubation for 1 h at RT with secondary antibodies coupled to horseradish peroxidase (ECL anti-mouse or -rabbit IgG; Amersham/GE Healthcare, Buckinghamshire, UK). The blots were developed using the SuperSignal enhanced chemiluminescence reagent (Pierce, Rockford, IL, USA) and exposed to Kodak X-OMAT film.

2.5. Mass-spectrometry analysis

The samples immunoprecipitated for full-length BRCA2 were subjected to SDS–PAGE, and the gels were stained with SYPRO Ruby Protein Gel Stain (Molecular Probes/Life Technologies, Carlsbad, CA, USA). The stained gel bands around 250 kDa were cut out and treated with dithiothreitol (DTT, Nacalai Tesque, Kyoto, Japan) dissolved in ammonium hydrogen carbonate (Nacalai Tesque), followed by treatment with iodoacetamide (Wako, Osaka, Japan). After the gels were dried, 20 μl of 0.05 pmol/μl trypsin (AB SCIEX, Framingham, MA, USA) solution was applied to each gel piece and incubated for 14 h at 37 °C to digest proteins. Digested peptides were extracted by washing the gel pieces twice with 50% trifluoroacetic acid (TFA, Wako), followed by washing with 80% TFA. The purified peptide samples were injected onto a reversed-phase C18 column (HiQ sil C18W-3P, 3 μm, 120 Å, KYA TECH Corp.) and separated by nanoflow liquid chromatography (300 nL/min) on a nano LC Dina-A system (KYA TECH Corp.) in line with a Q-TRAP 5500 instrument (AB SCIEX). A synthesized peptide that is recognized by MT-MMP1 (LSNNLNVEGG) and a mutant derivative (LSNNDNVEGG) were subjected to similar analysis following digestion.

2.6. Immunofluorescence (IF) analysis

HeLa S3 cells were fixed for 10 min on ice in 3.7% formaldehyde in PBS, and then sequentially permeabilized by incubation in 50%, 75%, and 95% ethanol solutions on ice for 5 min each. Slides were blocked with PBS containing blocking solution for 30 min at RT, incubated with primary antibody for 1 h at RT, and then washed three times with PBS. Next, cells were incubated with Alexa Fluor 488- or Alexa Fluor 594- conjugated secondary antibody (Molecular Probes; Life Technologies) for 1 h at RT, washed three times with PBS, and preserved in Vectashield (Vector Inc., Burlingame, CA, USA).

2.7. FACS analysis

HeLa cells were arrested at S phase by DTB. At various times, cells were washed with PBS, and then fixed in 70% ethanol solution. Fixed cells were washed twice with PBS, and then treated with RNase A at 37 °C for 30 min. Finally, cells were stained with propidium iodide and incubated in the dark for 30 min. Samples were analyzed by flow cytometry using fluorescence activated cell sorting (FACS, BD Bioscience, San Jose, CA). A total of 10,000 cells were counted for each sample. Gating of cell populations and quantitation were performed using the ModFit LT™ program provided by the Verity Software House.

2.8. MT1-MMP activity assay

MT1-MMP activity buffer was 50 mM Tris–HCl (pH 7.4), 150 mM NaCl, 1 mM $CaCl_2$, and 5 μM $ZnCl_2$. Recombinant MT1-MMP catalytic domain and Brij 35 (final concentration: 0.01%) were added to the activity buffer. Anti-HA or anti-FLAG immunoprecipitates from HeLa S3 cells expressing HA-BRCA2 or BRCA2-FLAG were incubated with 100 ng active MT1-MMP for 3 h at 37 °C, followed by immunoblotting with anti-HA or FLAG antibodies. Recombinant MT1-MMP catalytic domain (475935) and a hydroxamate inhibitor (GM6001, N-[(2R)-2-(hydroxamidocarbonylmethyl)-4-methylpentanoyl]-L-tryptophan methylamide) were purchased from CALBIOCHEM (USA). GM6001 was dissolved at a concentration of 25 mM in DMSO.

2.9. Knockdown of BRCA2 and MT1-MMP

Expression of BRCA2 was knocked down using two different siRNAs, BRCA2-1 (5′-GAAACGGACUUGCUAUUUA-3′) and BRCA2-2 (5′-GAAGAAUGCAGGUUUAAUA-3′). Likewise, MT1-MMP was knocked down using two different siRNAs, MT1-MMP-1 (5′-GGAUGGAC ACGGAGAAUUU-3′) and MT1-MMP-2 (5′-GGUCUCAAAUGGCAAC AUA-3′). Cells at about 40% confluence were transfected with siRNAs using Lipofectamine RNAiMAX reagent (Invitrogen; Life Technologies) in Opti-MEM I (Invitrogen; Life Technologies) and cultured in 5% CO_2 at 37 °C for 72 h.

3. Results

3.1. Detection of cleaved BRCA2 in cancer cells

The positions of the binding sites of BRCA2 antibodies are summarized in Fig. 1A. Using the antibodies Ab123491, Ab-1, and 5.23, full-length BRCA2 (384 kDa) was detected in several cell lines (Fig. 1B; lanes 1–6). Simultaneously, an approximately 250-kDa protein was also detected in cell lines other than MCF-7 using the Ab123491 and Ab-1 antibodies (Fig. 1B; lanes 1–5). By contrast, no 250-kDa protein was detected using the 5.23 antibody (Fig. 1B; lane 6). In order to confirm whether the 250-kDa protein was derived from BRCA2, we made use of specific BRCA2 siRNAs and the Ab123491 antibody. Fig. 1C shows that siRNAs against BRCA2 specifically reduced the level of full-length BRCA2 (384 kDa) and also significantly reduced the level of the 250-kDa protein, as revealed by immunoblotting for BRCA2. To further confirm the identity of the 250-kDa protein, anti-BRCA2 immunoprecipitate was subjected to SDS–PAGE followed by SYPRO RUBY staining, and the 250-kDa region of the gel was cut out and subjected by nano-LC–MS/MS. The mass-spectrometry analysis detected both BRCA2 and MT1-MMP (Fig. 1D). These results suggest the presence of a cleaved fragment of BRCA2 in several cancer cell lines.

3.2. MT1-MMP cleaves BRCA2

Searching the MEROPS peptidase database revealed the presence of four MT1-MMP cleavage sites (LSG402-L403, SHN1333-L1334, SDN1619-L1620 and SNN2135-L2136) in BRCA2 (Fig. 2A). Calculation of the molecular weights of fragments resulting from the predicted cleavage pattern identified two candidates for the 250-kDa protein described in the previous section (Fragment 1: 239-kDa and Fragment 2: 235-kDa). In order to narrow down the location of the MT1-MMP target cleavage site within BRCA2, we constructed a plasmid for expression of an HA-tagged fragment of BRCA2, HA-BRCA2 (a.a. 1596–2280), which includes the cleavage site, SNN^{2135}-L^{2136}. HA-BRCA2 purified on an HA-affinity column was cleaved into two fragments by active MT1-MMP, and one of the fragments was detected at 62 kDa (Fragment 3) using anti-HA antibody (Fig. 2A and B). When GM6001, an MMP inhibitor, was added to the cleavage reaction, the 62-kDa cleavage fragment was not observed (Fig. 2C). Furthermore, we observed a time-dependent increase in the level of Fragment 3, and a corresponding decrease in level of the original HA-BRCA2, following addition of active MT1-MMP (Fig. 2D). Next, we investigated whether full-length BRCA2 is cleaved by MT1-MMP. Full-length

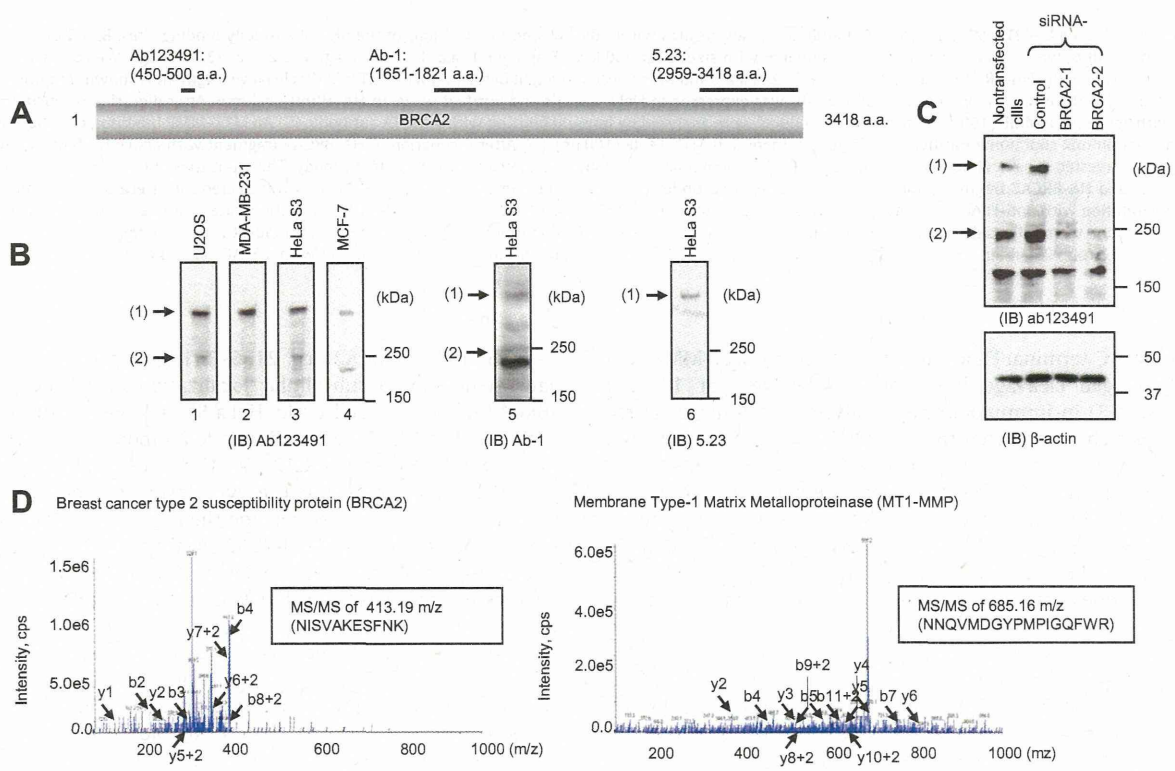

Fig. 1. A BRCA2 fragment of approximately 250 kDa was found in cancer cells and confirmed by mass spectrometry. (A) Schematic of epitope regions for three anti-BRCA2 antibodies. (B) Cell lysates from the indicated cell lines (U2OS, MDA-MB-231, HeLa S3, and MCF-7) were subjected to SDS–PAGE and blotted onto membranes. The blots were probed with antibodies (Ab123491, Ab-1, and 5.23) against BRCA2. Full-length BRCA2 (1) and a BRCA2 fragment of approximately 250 kDa (2) were detected by anti-BRCA2 antibody. (C) HeLa S3 cells were transiently transfected with BRCA2 siRNA (1 or 2), control siRNA, or nontransfected. At 72 h, cells were harvested and subjected to immunoblotting using anti-BRCA2 and anti-β-actin. β-actin was used as a gel loading control. (1) and (2) show full-length BRCA2 and the BRCA2 fragment of approximately 250 kDa, respectively. (D) Anti-BRCA2 and anti-IgG immunoprecipitates were subjected to SDS–PAGE, and the gel was stained with SYPRO RUBY. Gel bands corresponding to approximately 250 kDa were cut out and analyzed by nano-LC MS/MS. Mass spectra for a BRCA2 peptide (a.a. 1435–1445; left panel) and an MT1-MMP peptide (a.a. 346–362; right panel).

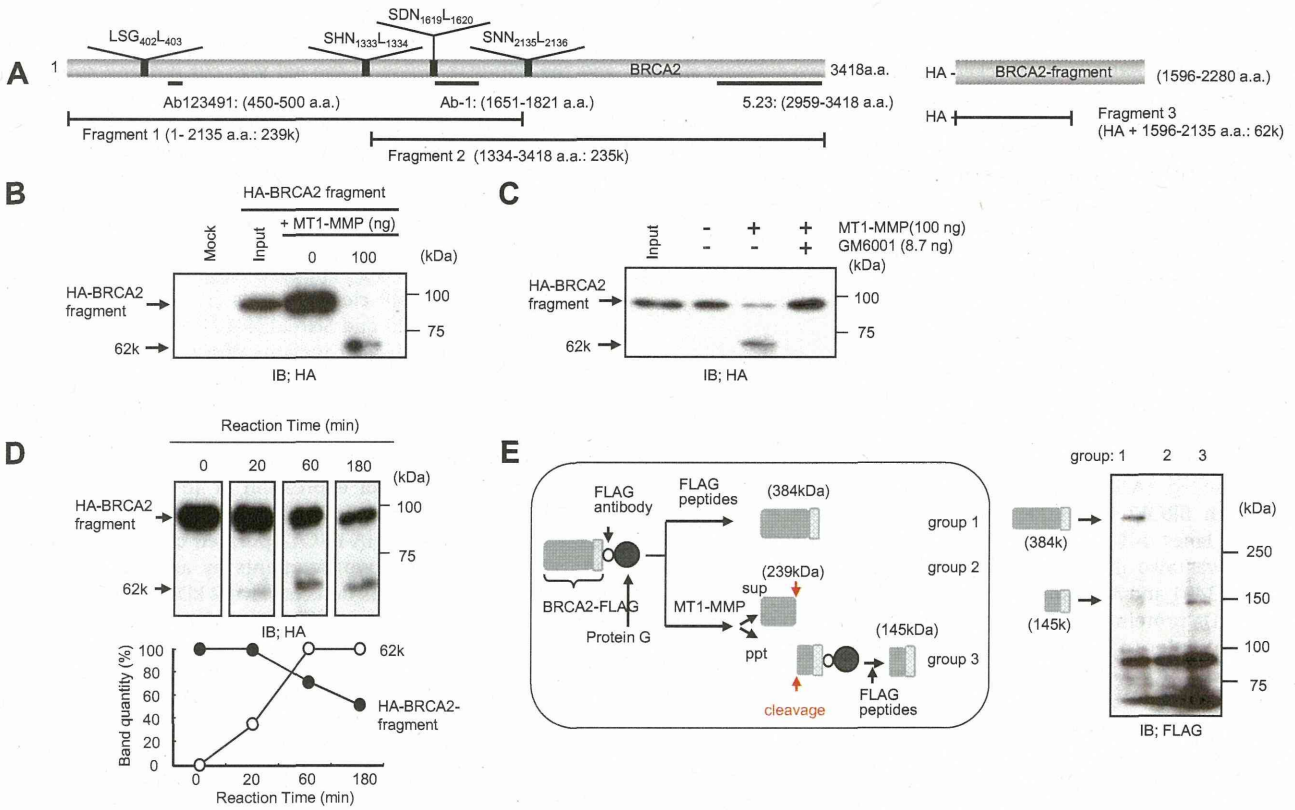

Fig. 2. BRCA2 is cleaved by MT1-MMP *in vitro*. (A) Candidate cleavage sites within BRCA2, and the positions of the BRCA2 antibody binding sites. Based on the positions of putative cleavage sites, we predicted two potential fragments with sizes near 250 kDa (Fragment 1: a.a. 1–2135; Fragment 2: a.a. 1334–3418). We constructed a plasmid vector for expression of the HA-BRCA2 fragment (a.a. 1596–2280 a.a.), and the molecular weight of the predicted MT1-MMP cleavage fragment is shown (Fragment 3: 62-kDa, a.a. 1596–2135). (B) HA-BRCA2 fragment (a.a. 1596–2280) was expressed in HeLa S3 cells and purified using an HA-affinity column. After digestion of purified HA-BRCA2 fragment with active MT1-MMP (100 ng), the reaction products were analyzed by immunoblotting with anti-HA antibody. (C) An MT1-MMP inhibitor, GM6001 (8.7 ng), was added to a reaction mix containing purified HA-BRCA2 fragment and MT1-MMP (100 ng). (D) After incubation of HA-BRCA2 fragment with active MT1-MMP, the digestion products were harvested at several points (0, 20, 60, and 180 min) and analyzed by immunoblotting with anti-HA antibody. The intensities of 62-kDa cleavage polypeptides (white circles) and HA-BRCA2 fragment (black circles) are indicated under the immunoblot image. (E) BRCA2-FLAG was transfected into HeLa S3 cells and collected by immunoprecipitation with anti-FLAG antibody. Precipitates were either not treated (group 1) or treated MT1-MMP1; from the treated samples, supernatant (group 2) and precipitate (group 3) were collected separately. All groups were subjected to SDS–PAGE and immunoblot with anti-FLAG antibody. Group 1 contains full-length FLAG-tagged BRCA2 (384 kDa); group 2 contains N-cBRCA2 without a FLAG tag (no band detected); and group 3 contains C-cBRCA2 with a FLAG tag (145 kDa).

BRCA2 with a C-terminal FLAG tag was cleaved by MT1-MMP, and the FLAG-tagged cleavage fragment was detected at 145 kDa (Fig. 2E, lane 3) in immunoblotting analysis. The other cleavage fragment, which is predicted to be a 239 kDa fragment lacking a FLAG tag, was not detected (Fig. 2E, lane 2).

To determine the MT1-MMP cleavage site within BRCA2 and to confirm the predictions based on the database search, we synthesized a 10-mer peptide (LSNNLNVEGG) derived from the putative cleavage site of BRCA2, and subjected it to cleavage by recombinant polypeptide corresponding to the catalytic domain of human MT1-MMP (abcam; ab38970). We determined the mass of the cleavage product (LNVEGG: 588.2 *m/z*) and the experimental MS/MS spectra by mass spectrometry (Supplemental Fig. S1). A mutant peptide containing a single amino-acid substitution, LSNN^{2135}-D^{2136}NVEGG (L2136D), was resistant to proteolysis by MT1-MMP (data not shown). These data further confirm that BRCA2, which bears the predicted cleavage site (LSNN2135↓L2136NVEGG), is cleaved by MT1-MMP.

3.3. Quantitative changes in C-cBRCA2 during the cell cycle

Next, we generated antibodies, brca2n and brca2c, that specifically recognize the cleavage fragments of BRCA2, N-cBRCA2 (a.a. 1–2135) and C-cBRCA2 (a.a. 2136–3418), respectively. To investigate in detail the subcellular localization of N-cBRCA2 and C-cBRCA2 during the cell cycle, HeLa S3 cells were immunostained with anti-BRCA2, brca2n, and brca2c antibodies (Fig. 3A). During interphase, full-length BRCA2 was localized to dots in the nucleus and widely distributed in the cytoplasm. In metaphase, BRCA2 was uniformly distributed outside the region containing the chromosomes. By contrast, N-cBRCA2 localized in the cytoplasm in interphase and metaphase, whereas C-cBRCA2 localized in the nucleus during interphase but was not detectable in metaphase (Fig. 3A).

Next, we examined the relationship between the levels of full-length and cleaved BRCA2. Fig. 3B shows a typical experiment in which cell-cycle progression was analyzed by flow cytometry up to 24 h after release from double-thymidine block (DTB). Cells were harvested at various times after release, and extracted proteins were analyzed on immunoblots using anti-BRCA2, brca2c, anti-MT1-MMP, and anti-βactin antibodies (Fig. 3C). The expression pattern of full-length BRCA2 was tightly regulated: its levels peaked in early S-phase, but decreased significantly by late S phase (Fig. 3D, left). By contrast, C-cBRCA2 was present throughout the cell cycle, with peak levels in late S phase. The level of MT1-MMP remained relatively constant throughout the cell cycle

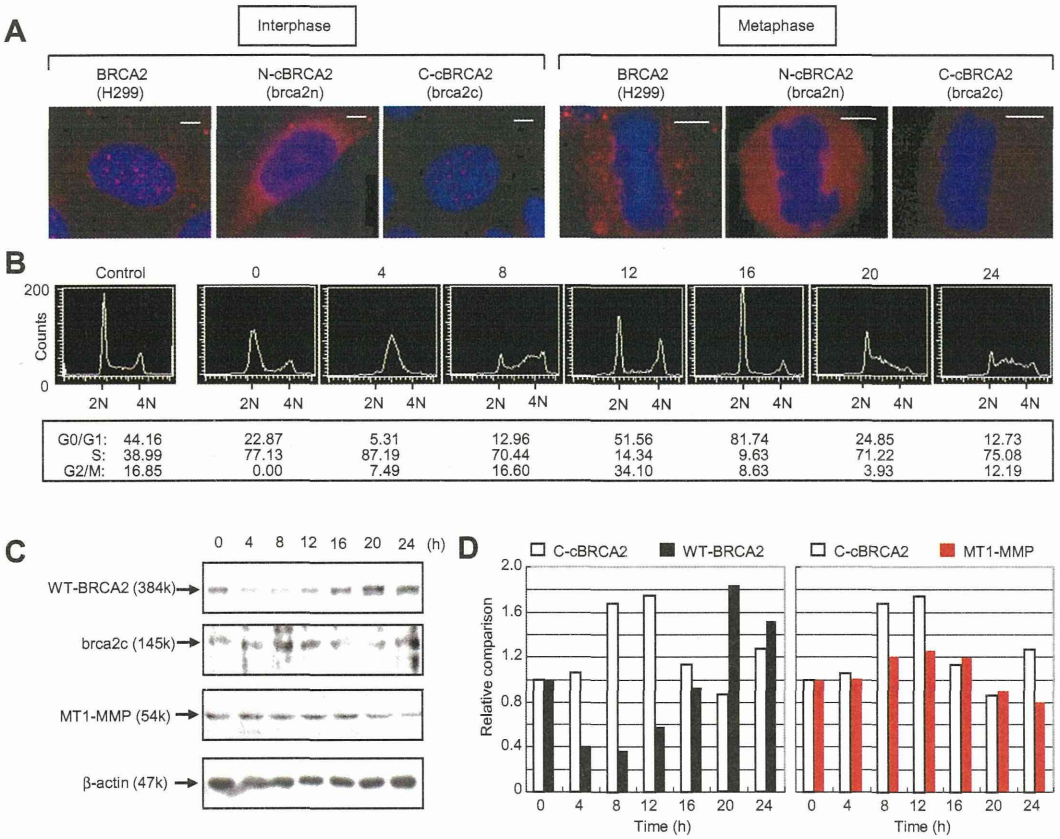

Fig. 3. Quantitative changes in the levels of full-length BRCA2 and C-cBRCA2 over the cell cycle. (A) HeLa S3 cells were fixed and stained for full-length BRCA2 with anti-BRCA2 (H299), for N-cBRCA2 with brca2n, or for C-cBRCA2 with brca2c, followed by staining with Alexa Fluor 594- conjugated anti-rabbit IgG (red). Nuclei are stained with Hoechst (blue). Bar, 5 μm. (B) FACS analysis illustrating the cell-cycle progression of synchronized HeLa S3 cells following release from double-thymidine block. Normal progression through the cell cycle (0 h for early S phase, 4 h for S phase, 8 h for late S to G2 phase, 12 h for G2/M to G0/G1 phase, 16 h for G1 phase, 20 h for late G1 to early S phase, and 24 h for S phase). (C) Total cell lysates were prepared after releasing cells from a double-thymidine-block. Equal quantities of protein from each lysate were subjected to SDS–PAGE followed by immunoblot analysis with anti-BRCA2, brca2c, anti-MT1-MMP, and anti-β-actin antibodies. (D) The column graph at left shows quantitations of full-length BRCA2 (black) and C-cBRCA2 (white) over the course of the cell cycle. The column graph at right shows quantitations of C-cBRCA2 (white) and MT1-MMP (red) over the course of the cell cycle.

(Fig. 3D, right). These results suggest that the levels of cleaved BRCA2 are inversely correlated to those of the full-length protein.

3.4. MT1-MMP cleaves BRCA2 in M phase

The localization of BRCA2 at centrosomes is stringently regulated throughout the cell cycle (Fig. 4A); however the mechanism by which BRCA2 gradually disappears from centrosomes during prophase remains unknown. We observed a marked increase in the level of cleaved BRCA2 during the transition between late S and early M phases (Fig. 3C and D). We hypothesized that the disappearance of BRCA2 from centrosomes could be attributed to cleavage by MT1-MMP. To test this idea, we immunostained cells treated with siRNA against MT1-MMP, or a control siRNA, with anti-BRCA2 and γ-tubulin antibodies, and observed by immunofluorescence microscopy the localization of BRCA2 at centrosomes in metaphase. Immunoblot analysis revealed upregulation of BRCA2 expression in MT1-MMP siRNA-treated cells relative to control siRNA-treated cells (Fig. 4B). Furthermore, as shown in Fig. 4C and D, the BRCA2 signal was stronger at centrosomes in MT1-MMP siRNA-treated cells than in control siRNA-treated cells. Fluorescence intensity profiles along lines drawn between centrosomes revealed the degree of centrosomal staining patterns. These results suggest that the disappearance of BRCA2 from centrosomes during mitosis can be attributed to proteolysis by MT1-MMP.

4. Discussion

The results of this study provide important information regarding BRCA2 proteolysis by MT1-MMP. We demonstrated that a peptide containing the putative cleavage site of BRCA2 (LSNN^{2135}-L^{2136}NVEGG) was cleaved by MT1-MMP (Supplemental Fig. S1), whereas a peptide containing the L2135D substitution was resistant to MT1-MMP. This cleavage site is compatible with the known cleavage preferences of MT1-MMP, and is supported by our biochemical experiments. Furthermore, as shown in Fig. 1B, no 250-kDa fragment of cleaved BRCA2 was detected in MCF-7 cells, which do not express MT1-MMP (Fig. 1B).

MT1-MMP, MMP2, and MMP-9 are associated with tumor invasion and metastasis in ovary [14] and breast carcinomas [15]. Substrates of these MMPs can be divided into four groups according to the selectivity of recognition [16], as follows: (I) substrates recognized by all three MMPs; (II) substrates recognized equally by MT1-MMP and MMP-2; (III) substrates recognized equally by MT1-MMP and MMP-9; and (IV) substrates recognized selectively by MT1-MMP. In this study, we could not determine whether the cleavage site sequence of BRCA2 belongs to any of these groups, because it does not exactly match reported sequences. However, in contrast to the other two MMPs, MT1-MMP is localized to the centrosome, as is the case with BRCA2 [17,10]. In addition, only MT1-MMP was identified in by mass

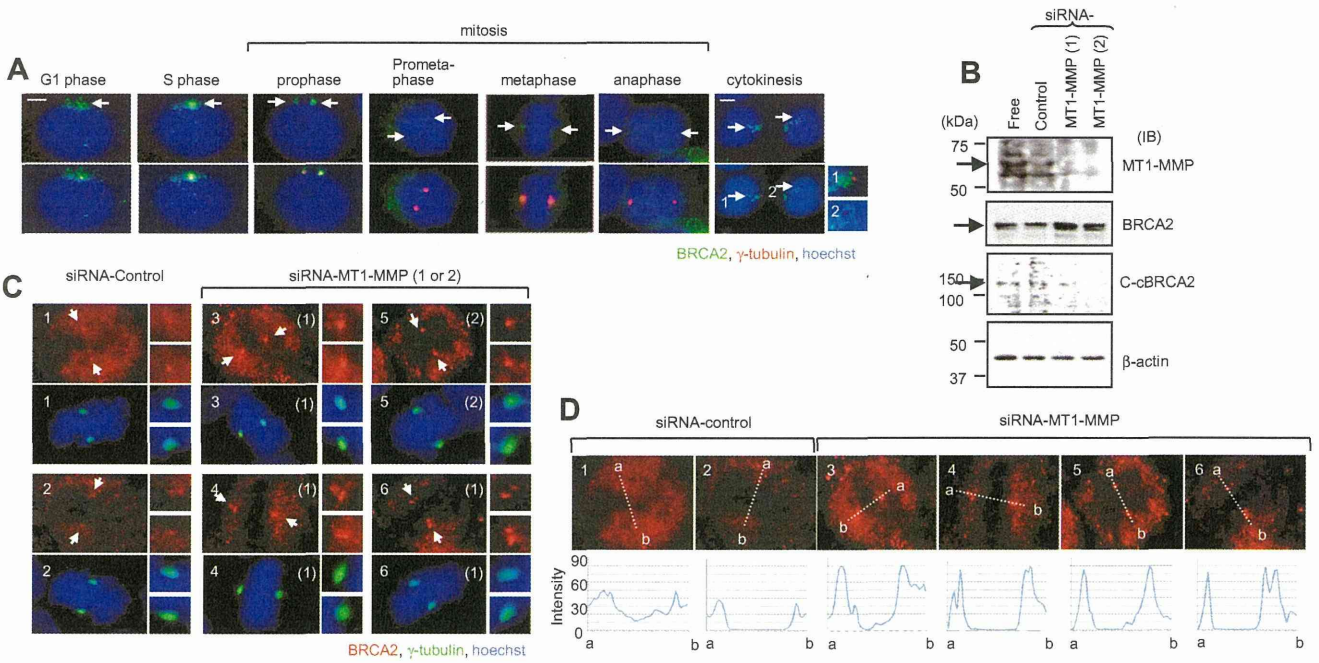

Fig. 4. Recovery of BRCA2 at centrosomes following siRNA knockdown of MT1-MMP. (A) Localization of full-length BRCA2 from G1 phase through cytokinesis. Full-length BRCA2 is green, γ-tubulin is red, and nuclear DNA (stained with Hoechst) is blue. Magnification of the centrosomal region is shown in the merged images (1 and 2). Scale bar is 5 μm. (B) HeLa S3 cells were transiently transfected with siRNA against MT1-MMP siRNA (1 or 2), control siRNA, or not transfected. After 72 h, cells were harvested and subjected to immunoblotting using anti-MT1-MMP, anti-BRCA2, brca2c, anti-β-actin antibodies. β-actin was used as a gel loading control. (C) Localization of BRCA2 in HeLa S3 cells treated with siRNA against MT1-MMP. Cells were fixed and immunostained with antibodies against BRCA2 (red) and γ-tubulin (green). Nuclei were stained with Hoechst (blue). (D) Line scans (from "a" to "b") measuring centrosome-associated relative fluorescence intensity were generated using the ImageJ software, and the traces are displayed below the corresponding images; lines represent BRCA2 fluorescence.

spectrometry analysis of anti-BRCA2 immunoprecipitates (Fig. 1D). Together, these results indicate that BRCA2 is cleaved by MT1-MMP.

What is the biological significance of BRCA2 cleavage by MT1-MMP? BRCA2 is localized on centrosomes between G1 phase and prophase, and it gradually disappears from the centrosomes over the course of mitosis; previously, the underlying mechanism was unknown. These dynamic changes were abrogated by siRNA-mediated knockdown of MT1-MMP. Furthermore, the level of a cleavage fragment of BRCA2, C-cBRCA2, increased in late S and G2/M phases in cells synchronized by DTB. This phenomenon may be related to the disappearance of BRCA2 from centrosomes in mitosis. One possibility is that BRCA2 is cleaved by MT1-MMP at centrosomes during mitosis, resulting in the disappearance of BRCA2 from centrosomes.

Overall, our data suggest that there is a causal link between MT1-MMP-mediated proteolysis of BRCA2 and the disappearance of BRCA2 from centrosomes during mitosis. We also suggest that MT1-MMP might serve as a cell cycle-associated regulator of BRCA2 that maintains the appropriate abundance of BRCA2 at centrosomes.

Acknowledgments

This work was supported by JSPS KAKENHI Grant Numbers 23650592 (Y.M.). We thank all members of Department of Molecular Genetics of Tokyo Medical and Dental University (TMDU).

Appendix A. Supplementary data

Supplementary data associated with this article can be found, in the online version, at http://dx.doi.org/10.1016/j.bbrc.2013.12.103.

References

[1] Breast Cancer Linkage Consortium, Cancer risks in BRCA2 mutation carriers, J. Natl. Cancer Inst. 91 (1999) 1310–1316.
[2] M. Goggins, M. Schutte, J. Lu, C.A. Moskaluk, C.L. Weinstein, G.M. Petersen, C.J. Yeo, C.E. Jackson, H.T. Lynch, R.H. Hruban, S.E. Kern, Germline BRCA2 gene mutations in patients with apparently sporadic pancreatic carcinomas, Cancer Res. 56 (1996) 5360–5364.
[3] S.C. Wang, R. Shao, A.Y. Pao, S. Zhang, M.C. Hung, L.K. Su, Inhibition of cancer cell growth by BRCA2, Cancer Res. 62 (2002) 1311–1314.
[4] A. Nakanishi, X. Han, H. Saito, K. Taguchi, Y. Ohta, S. Imajoh-Ohmi, Y. Miki, Interference with BRCA2, which localizes to the centrosome during S and early M phase, leads to abnormal nuclear division, Biochem. Biophys. Res. Commun. 355 (2007) 34–40.
[5] M.J. Daniels, Y. Wang, M. Lee, A.R. Venkitaraman, Abnormal cytokinesis in cells deficient in the breast cancer susceptibility protein BRCA2, Science 306 (2004) 876–879.
[6] L.K. Su, S.C. Wang, Y. Qi, W. Luo, M.C. Hung, S.H. Lin, Characterization of BRCA2: temperature sensitivity of detection and cell-cycle regulated expression, Oncogene 17 (1998) 2377–2381.
[7] A.C. Carrano, E. Eytan, A. Hershko, M. Pagano, SKP2 is required for ubiquitin-mediated degradation of the CDK inhibitor p27, Nat. Cell Biol. 1 (1999) 193–199.
[8] L. Moro, A.A. Arbini, E. Marra, M. Greco, Up-regulation of Skp2 after prostate cancer cell adhesion to basement membranes results in BRCA2 degradation and cell proliferation, J. Biol. Chem. 281 (2006) 22100–22107.
[9] S. Zucker, D. Pei, J. Cao, C. Lopez-Otin, Membrane type-matrix metalloproteinases (MT-MMP), Curr. Top. Dev. Biol. 54 (2003) 1–74.
[10] V.S. Golubkov, S. Boyd, A.Y. Savinov, A.V. Chekanov, A.I. Osterman, A. Remacle, D.V. Rozanov, S.J. Doxsey, A.Y. Strongin, Membrane type-1 matrix metalloproteinase (MT1-MMP) exhibits an important intracellular cleavage function and causes chromosome instability, J. Biol. Chem. 280 (2005) 25079–25086.
[11] V.S. Golubkov, A.V. Chekanov, S.J. Doxsey, A.Y. Strongin, Centrosomal pericentrin is a direct cleavage target of membrane type-1 matrix metalloproteinase in humans but not in mice: potential implications for tumorigenesis, J. Biol. Chem. 280 (2005) 42237–42241.
[12] N.D. Rawlings, A large and accurate collection of peptidase cleavages in the MEROPS database, Database (Oxford) 2009 (2009) bap015.

[13] N.D. Rawlings, A.J. Barrett, A. Bateman, MEROPS: the database of proteolytic enzymes, their substrates and inhibitors, Nucleic Acids Res. 40 (2012) D343–50.
[14] K. Sakata, K. Shigemasa, N. Nagai, K. Ohama, Expression of matrix metalloproteinases (MMP-2, MMP-9, MT1-MMP) and their inhibitors (TIMP-1, TIMP-2) in common epithelial tumors of the ovary, Int. J. Oncol. 17 (2000) 673–681.
[15] J.L. Jones, P. Glynn, R.A. Walker, Expression of MMP-2 and MMP-9, their inhibitors, and the activator MT1-MMP in primary breast carcinomas, J. Pathol. 189 (1999) 161–168.
[16] S.J. Kridel, H. Sawai, B.I. Ratnikov, E.I. Chen, W. Li, A. Godzik, A.Y. Strongin, J.W. Smith, A unique substrate binding mode discriminates membrane type-1 matrix metalloproteinase from other matrix metalloproteinases, J. Biol. Chem. 277 (2002) 23788–23793.
[17] Y.C. Ip, S.T. Cheung, S.T. Fan, Atypical localization of membrane type 1-matrix metalloproteinase in the nucleus is associated with aggressive features of hepatocellular carcinoma, Mol. Carcinog. 46 (2007) 225–230.